

Shot noise does not always provide the quasiparticle charge

Received: 23 December 2021

Accepted: 16 August 2022

Published online: 29 September 2022

 Check for updates

Sourav Biswas¹, Rajarshi Bhattacharyya^{1,4}, Hemanta Kumar Kundu¹, Ankur Das², Moty Heiblum¹✉, Vladimir Umansky¹, Moshe Goldstein³ and Yuval Gefen²

The fractional charge of quasiparticles is a fundamental feature of quantum Hall effect states. The charge—important in characterizing the state and in interference experiments—has long been measured via shot noise at moderate temperatures, with the Fano factor revealing the charge of the quasiparticles. However, at sufficiently low temperatures of ~10 mK, we previously found that the Fano factor is instead equal to the bulk filling factor. Noise with this pattern was also observed on intermediate conductance plateaux in the transmission of the quantum point contact, where shot noise is not expected. Here, we extend this low-temperature behaviour of the Fano factor to a situation where the edge modes do not sit at the physical edge of the device but instead reside in an artificially constructed interface at the boundary between two adjoining quantum Hall effect states: the tested state and a different state. We attribute the unexpected shot noise behaviour to upstream neutral modes that proliferate at the lowest spinless Landau level. We present a theoretical approach based on an interplay between charge and neutral modes that hints at the origin of the universal Fano factor.

One of the key fundamental measurements in mesoscopic quantum transport is determination of the quasiparticle charge¹. Quantum shot noise has been the most reliable means for revealing this charge. By employing this approach, quasiparticle charge has been measured in quantum Hall systems², Josephson junctions³ and superconductors^{4,5}. Shot noise measurements are yet to be performed in emerging exotic states such as the anomalous quantum Hall effect⁶ and in fractional Chern insulators⁷ in two-dimensional (2D) topological systems⁸.

The quantum Hall effect (QHE) is the oldest known topological quantum system^{9,10}. The most natural description of its gapped bulk is understood via the so-called Landau levels (LLs), which host localized quasiparticles, with different topological phases described by the filling factor (ν). Although the bulk is insulating, the low-energy dynamics is governed by gapless chiral edge modes^{11–14},

which carry current and energy. ‘Bulk–edge’ correspondence dictates that both the Hall conductance σ_{xy} and the thermal Hall conductance K_{xy} are determined by the topological order of the bulk¹⁵. The quasiparticle charge, e^* , being the most fundamental quantity of a fractional state, is crucial in determining quasiparticle statistics (in interference experiments)¹⁶.

According to the orthodox paradigm, weak partitioning of edge modes, done in a quantum point contact (QPC) constriction, leads to shot noise with a Fano factor $F = e^*/e$ ($F = 1$ for integers)^{17–19}. Moreover, shot noise (at zero temperature) should be zero on an intermediate conductance plateau of the QPC, as modes are either fully transmitted or fully reflected; that is, there is no intra-mode partitioning. Indeed, early on, experimental results performed at moderate temperatures of $T > 30$ mK adhered to this expectation^{20–23}.

¹Braun Center for Submicron Research, Department of Condensed Matter Physics, Weizmann Institute of Science, Rehovot, Israel. ²Department of Condensed Matter Physics, Weizmann Institute of Science, Rehovot, Israel. ³Raymond and Beverly Sackler School of Physics and Astronomy, Tel-Aviv University, Tel Aviv, Israel. ⁴Present address: Department of Physics, University of California, San Diego, La Jolla, CA, USA.

✉e-mail: moty.heiblum@weizmann.ac.il

However, in more recent shot noise measurements, performed at $T \approx 10$ mK, we found^{24–26} (1) non-zero noise on intermediate conductance plateaux with the partitioning QPC and (2) that the Fano factor is equal to the filling factor in the bulk (away from the QPC), on and off the intermediate conductance plateaux within a QPC. These observations necessitate further investigation and a new understanding beyond the orthodox paradigm.

In this Article, to demonstrate the universality of the Fano factor, we employ a method in which two different states are interfaced, giving birth to 1D interface modes at the boundary between the two adjoined states. These modes do not obey ‘bulk–edge’ correspondence, having a different effective filling (conductance) than the bulk and QPC fillings.

It has already been demonstrated that upstream (US) neutral edge modes proliferate in many QHE states in the lowest LL^{26–28}. These modes can be topological (determined by the bulk) or emergent due to spontaneous edge reconstruction^{28,29}. Here, we show that neutral modes play a crucial role in generating (partitioned) shot noise. The new paradigm of shot noise generation consists of a two-step process: inter-mode charge equilibration (between ‘hot’ and ‘cold’ modes), accompanied by excitation of neutral quasiparticles and subsequent annihilation of these ‘neutralons’. This process leads to stochastic generation of quasiparticle/quasihole pairs, resulting in shot noise. We show that the latter is characterized by a Fano factor that is equal to the bulk filling factor. Notably, the Fano factor does not depend on the edge-mode structure (and its conductance) and not on the local filling within the QPC constriction (if not too small).

Past results and our measurement platform

Past results

Early shot noise measurements, performed at $\nu = 1/3$ and $\nu = 2/5$ particle states at moderate temperatures ($T > 25$ mK), led to $F \approx 1/3$ and $F \approx 1/5$, respectively^{20,22}. However, later measurements with $\nu = 2/5$ and $\nu = 3/7$, performed at lower temperatures ($T < 15$ mK), approached $F \approx \nu_b$ (ref.²⁴). Increasing the temperature led to $F \approx 1/5$ and $F \approx 1/7$, respectively. Similarly, low-temperature measurements in particle–hole conjugated states, $\nu = 2/3$, $\nu = 3/5$ and $\nu = 4/7$, measured on and off the QPC intermediate plateaux, resulted in $F \approx \nu_b$ (refs.^{25,26}). At $\nu = 2/3$, with increased temperature, $F \approx 1/3$ with $e^* = e/3$ quasiparticle charge was obtained²⁵. Observation of noise on an intermediate conductance plateau thus necessitates overhauling the existing paradigm of shot noise.

Consider first the example of $\nu = 1/3$ bulk filling. The conventional picture of the edge structure comprises one downstream (DS) charged mode. However, edge reconstruction³⁰, taking place when the edge confining potential is not steep, may lead to pairs of additional $\nu = 1/m$ counter-propagating modes (where m is an odd integer). This is similar to the reconstruction of the $\nu = 2/3$ and the $\nu = 1$ edge with $m = 3$ (refs.^{25,26,31–34}). Accounting for an interplay of inter-mode Coulomb interactions and disorder-induced tunnelling, a new fixed point that features neutral mode(s) settles in^{29,35}: two DS charged modes and one US neutral mode, keeping K_{xy} unchanged. In a similar way, with edge reconstruction, $\nu = 2/5$ constitutes three DS charged modes and one US neutral mode. The unreconstructed edge will support two conventional DS charged modes, an inner $\nu = 1/5$ and an outer $\nu = 1/3$. Our paradigm for the reconstructed shot noise relies on excited US neutral modes due to charge equilibration between the hot charge modes that emanate from the biased source and the cold charge modes emanating from the grounded contact^{33,34,36}. Moving upstream, the neutral modes decay, generating randomized charged quasiparticle/quasihole pairs on different charge modes. Each of the pairs splits, with the quasiparticles (quasiholes) arriving at drain D1 (where the noise is measured; Fig. 2a) and the quasiholes (quasiparticles) at drain D2. This adds a stochastic component to the current measured in D1.

The mechanism described here (details are provided in the following) goes beyond the partitioned beam paradigm for shot noise.

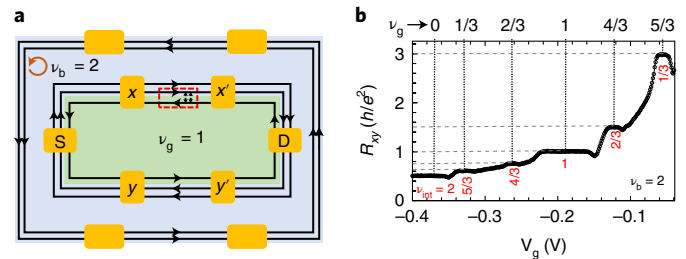


Fig. 1 | Interface edge modes. **a**, Schematic of the platform with top gated bulk with filling $\nu_g = 1$ state (green). The ungated surrounding region is at $\nu_b = 2$ (blue). Counter-propagating interface edge modes are equilibrated with an effective filling of $\nu_{\text{int}} = \nu_b - \nu_g$. Source contact S and drain contact D (yellow) are located at the interface. The x and y contacts are used to measure the four-probe Hall conductance, $\sigma_{xy} = \nu_{\text{int}} \frac{e^2}{h}$ of the interface edge. **b**, Interface Hall resistance for $\nu_b = 2$ as a function of the centre gate voltage (filling factor of the centre bulk), showing the integer and fractional plateaux of the interface modes.

It only assumes complete decay of the excited neutral modes in the course of equilibration. The number of those (equal to the number of stochastically generated quasiparticle/quasihole pairs) is defined by the filling of the bulk away from the QPC.

The platform

To further reaffirm the universality of the Fano factor, we exploit a fabrication method that allows us to interface a tested state with bulk filling ν_b with an adjacent (gate-controlled) state ν_g . The resultant interface mode, with an effective filling $\nu_b - \nu_g$, is partitioned by a QPC with its own shot noise, where bulk–edge correspondence is not valid. This shot noise is compared with the ubiquitous shot noise of partitioned edge modes.

Our playground is a standard molecular-beam-epitaxy-grown GaAs–AlGaAs heterostructure harbouring high-mobility two-dimensional electron gas, located 86 nm below the surface, with an electron density of $1.7 \times 10^{11} \text{ cm}^{-2}$. Electrical measurements were carried out at the electron base temperature of 12–14 mK.

The deployed platform is shown in Fig. 1a. A gate-defined Hall bar with filling ν_g (green) is embedded in the bulk of a mesa with filling ν_b (light blue). If $\nu_g < \nu_b$, an equilibrium interface mode circulates the Hall bar with an effective filling of $\nu_{\text{int}} = \nu_b - \nu_g$ and conductance $G = \nu_{\text{int}} \frac{e^2}{h}$, measured between ohmic contacts (yellow) placed at the formed interface. In the example of Fig. 1a, with $\nu_{\text{int}} = 2 - 1 = 1$, only the inner integer mode participates in transport.

Figure 1b shows the Hall resistance R_{xy} of the gated region as a function of the gate voltage V_g , with $\nu_b = 2$. As $V_g \rightarrow 0$ V, $R_{xy} \rightarrow \infty$ (the interface vanishes). For $V_g < -0.35$ V, the gated region is fully depleted and $R_{xy} = \frac{h}{2e^2}$. Five conductance plateaux in units of $\frac{e^2}{h}$ are observed $(\frac{1}{3}, \frac{2}{3}, 1, \frac{4}{3}, \frac{5}{3}, 2)$, assuring charge equilibration³⁷ at the interface.

Noise measurements

Shot noise was measured by partitioning the interface modes (Fig. 2a). The QPC constriction was formed by the lower and upper gated regions. The spectral density of the charge fluctuations was filtered by an LC resonant circuit with centre frequency of 937 kHz and bandwidth of 30 kHz. A high-electron-mobility transistor-based preamplifier cooled to 4 K (with voltage noise on the order of 300 pV $\text{Hz}^{-1/2}$ and current noise on the order of 10 fA $\text{Hz}^{-1/2}$) was cascaded by a room-temperature amplifier (with voltage noise on the order of 0.5 nV $\text{Hz}^{-1/2}$), feeding a spectrum analyser.

The general expression for the low-frequency spectral density of the shot noise is $S_r(0) = 2FeI_{\text{dc}}t(1-t)\left\{\coth\left(\frac{FeV}{2k_B T}\right) - \frac{2k_B T}{FeV}\right\}$, where t is the transmission of the QPC, $I_{\text{dc}} = V_{\text{DS}}G$ is the impinging current,

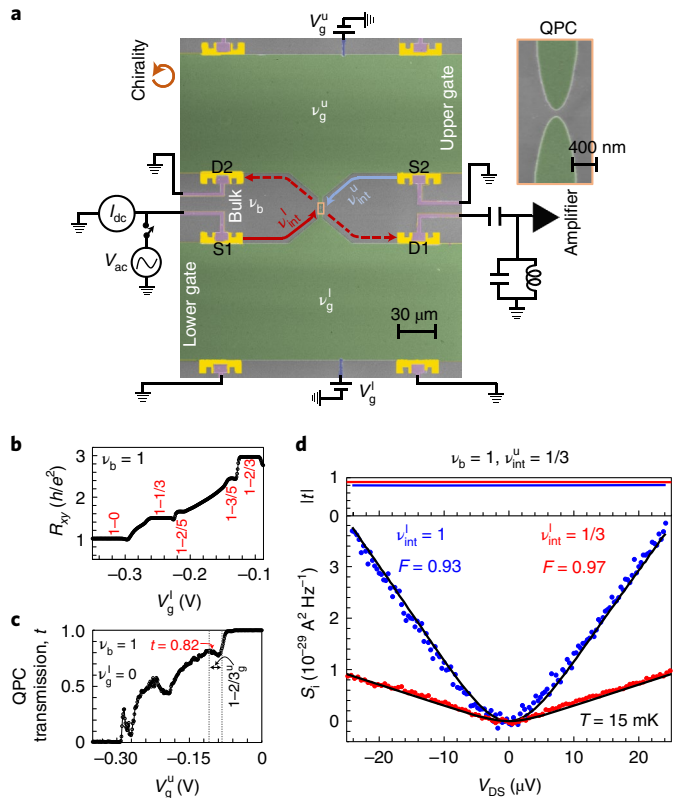


Fig. 2 | Experimental set-up for shot noise measurement with interface modes. **a**, False-colour scanning electron microscopy image of the QPC geometry formed by two peninsulas of two separate gates. Inset: enlarged image of the QPC. The ohmic contacts (yellow) were made by alloying Au/Ge/Ni, and the gates (green) were formed by evaporating a thin PdAu/Au film on top of a 25-nm layer of atomic-layer-deposited HfO₂. Metallic air bridges (dark blue) are connected to the gates to apply gate voltage. Source contact S1 (connected to the d.c. bias) and drain contact D1 (connected to the amplifier) are located at the lower gate interface. A d.c. voltage V_g^l sets the filling factor underneath, and thereby the incoming interface mode. The gate voltage V_g^u on the upper gate tunes the QPC backscattering but does not guarantee the filling underneath to be the same as in the lower gate. Hot (biased) and cold (grounded) edge modes are shown in red and light-blue lines, respectively. The source–QPC distance is $\sim 50 \mu\text{m}$, and charge equilibration at the interface is established within a few micrometres. **b**, Four-terminal conductance measurements as a function of V_g^l , showing the formation of fractional edge modes around the lower gate at $\nu_b = 1$. **c**, QPC transmission t as a function of V_g^l , with V_g^u fixed such that $\nu_g^l = 0$; that is, the incoming edge mode is $1 - 0$. The red arrow indicates t for the shot noise when $\nu_g^l = 2/3$; that is, the upper mode is $1 - 2/3$. **d**, Measured Fano factors for $I_b - 0_g = 1_{\text{int}}$ and $I_b - 2/3_g = 1/3_{\text{int}}$ interface modes. The top panel shows bias-dependent QPC transmission, where $t \approx 0.82$ for 1_{int} (blue) and $t \approx 0.88$ for $1/3_{\text{int}}$ (red). The bottom panel shows the measured spectral density S_I of DS current fluctuation with V_{DS} (that is, $I_{\text{dc}} \times R_{\text{xy}}$), shown as symbols. The black solid line is the fit. For both $I_b - 0_g = 1_{\text{int}}$ (blue) and $I_b - 2/3_g = 1/3_{\text{int}}$ (red), the Fano factor is $F \approx 1$. Estimated Fano factors have an accuracy of within ± 0.05 . The obtained electron temperature is 15 mK.

and k_B is the Boltzmann constant^{25,38–41}. The gain is calibrated by measuring the shot noise at weak backscattering of the outer edge mode in the $2 - 0$ configuration, with an expected $F = 1$. The detailed procedure for the analysis is described in Supplementary Section I.

Results

We generalize the ubiquitous noise measurements by presenting the key results for the partitioning interface modes. We control the lower (upper) interface mode with an effective filling of ν_{int}^l (ν_{int}^u) (Fig. 2a), with bulk filling ν_b . We test (1) different (incoming) modes' fillings at

Table 1 | Measured Fano factors for different configurations when $\nu_b = 1$

Mode configuration	Bulk ν_b	Lower mode $\nu_{\text{int}}^l = \nu_b - \nu_g^l$	Upper mode $\nu_{\text{int}}^u = \nu_b - \nu_g^u$	Transmission (t) and Fano factor (F)
Integer modes	1	1	1	$t \approx 0.60$, $F = 0.93$ (Extended Data Fig. 1a)
Integer and fractional	1	1	1/3	$t \approx 0.80$, $F = 0.93$ (Fig. 2d, blue plots)
Fractional modes symmetric	1	1/3	1/3	$t \approx 0.88$, $F = 0.97$ (Fig. 2d, red plots)
Fractional modes asymmetric	1	1/3	2/5	$t \approx 0.91$, $F = 1.0$ (Extended Data Fig. 1b)
Asymmetric	1	1/3	Not quantized	$t \approx 0.90$, $F = 1.0$ (Extended Data Fig. 1b)

Table 2 | Measured Fano factors for different configurations when $\nu_{\text{int}}^l = 2/3$

Bulk configuration	Bulk ν_b	Lower mode $\nu_{\text{int}}^l = \nu_b - \nu_g^l$	Upper mode $\nu_{\text{int}}^u = \nu_b - \nu_g^u$	Transmission (t) and Fano factor (F)
Integer bulk	1	2/3	1/3	$t \approx 0.50$, $F = 1.0$ (Fig. 3a, red plots)
Fractional bulk	2/3	2/3	1/3	$t \approx 0.50$, $F = 0.64$ (Fig. 3a, blue plots)

a fixed bulk filling and (2) a fixed incoming mode filling at different bulk fillings.

Fixed $\nu_b = 1$

The conductance showing fractional modes at the lower interface is plotted as a function of the lower gate voltage, V_g^l , in Fig. 2b. An example of tuning the QPC transmission with V_g^l when the lower gated region is depleted and $\nu_{\text{int}}^l = 1$ is shown in Fig. 2c. The desired upper mode ν_{int}^u is set by a V_g^u that also sets a transmission t for the incoming mode ν_{int}^l . The observed results for the Fano factor with different modes' filling are summarized in Table 1. In all cases, $F \approx 1$. Note that uncertainty in the exact electron temperature and the slight nonlinearity of the transmission lead to the deviations from $F = 1$.

Fixed $\nu_{\text{int}}^l = 2/3$

Two types of 'electron–hole conjugated' interfaced mode, $\nu_{\text{int}}^l = I_b - 1/3_g = 2/3_{\text{int}}$ and $2/3_b - 0_g = 2/3_{\text{int}}$ are tested. Edge reconstruction leads to two DS co-propagating $1/3$ modes joined by two US neutral modes (Supplementary Section II)^{29,34}. An intermediate conductance plateau is observed within the QPC at $t = 0.5$ (Extended Data Fig. 2). The fully transmitted outer $1/3$ mode and the fully reflected inner $1/3$ mode do not lead to shot noise. However, the observed noise on the $t = 0.5$ plateau, resulting from fractionalization of the neutral modes, leads to a Fano factor that is equal to the bulk filling factor (Table 2).

The Fano factor remains close to the bulk filling for a wide range of QPC transmissions, that is, away from the conductance plateau (Fig. 3b). When the QPC is strongly pinched, quasiparticle bunching⁴² leads to $F \approx 1$ at a lower bias in all cases (Extended Data Fig. 3). Extended Data Fig. 4 presents more data for interface fractional edge modes $2/3_b - 1/3_g = 1/3_{\text{int}}$ and $2/3_b - 4/15_g = 2/5_{\text{int}}$, with $F \approx \nu_b$, and Supplementary Section III provides additional measured data.

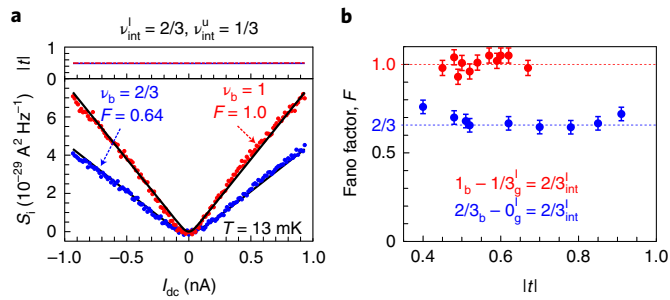


Fig. 3 | Shot noise with two types of interface 2/3 mode ($1 - 1/3$ and $2/3 - 0$). **a**, Shot noise measurements at $1_b - 1/3_g = 2/3_{\text{int}}$ and $2/3_b - 0_g = 2/3_{\text{int}}$ on the plateau of $t = 1/2$. Top: bias dependence of the transmission. Bottom: excess noise data at $1_b - 1/3_g$ (red symbols) and at $2/3_b - 0_g$ (blue symbols) with I_{dc} . Black solid lines are the fits, with the appropriate Fano factors. **b**, The Fano factor is equal to bulk filling, measured over a wide range of QPC transmission. The accuracy, estimated by the standard deviation of the measured Fano factor, is within ± 0.04 for both cases. This standard deviation is added to the data points as error bars.

Theoretical model and discussion

Our theoretical paradigm relies on the ubiquitous presence of counter-propagating neutral modes in the lowest spinless LL, being topological (for particle–hole conjugated states) or born due to spontaneous edge reconstruction (for integer and particle-like states)^{26,28,30,33} when the confining potential at the physical edge is not perfectly sharp^{43,44}.

We chose to consider here the simplest example of a reconstructed $\nu = 1/3$ bulk filling²⁸ in the orthodox QPC geometry, as this treatment captures the main physics of the universality of quantum shot noise. In a general case, we assume the formation of a single $1/m$ fractional strip at the edge of the 2D bulk, with two counter-propagating $1/m$ modes (Fig. 4a,b). Accounting for inter-mode interaction and tunnelling, the modes' structure, shown in Fig. 4b, renormalizes into two DS modes with charge $(1/3 - 1/m)e$ and e/m (from the inner to the outer) and a US neutral mode (Fig. 4c)^{29,35}. In Fig. 4d, we plot the DS hot charge modes that emanate from the biased source S1 (solid lines), while the DS cold modes emanate from the grounded S2 (broken lines). Source S1 injects N quasiparticles into each mode in a time interval τ (total current from source $I_{\text{dc}} = Ne/3\tau$). With the QPC tuned to partition a fraction f of the outermost $1/m$ charge mode, its total transmission is $t = 3(1 - f)/m$.

On the way to D1 and D2, the hot and cold modes equilibrate to the same chemical potential. The equilibration process keeps the currents arriving at the respective drains unchanged. Following this equilibration, the number of quasiparticles in each mode is $N_1 = (1 - f)3N/m$ near D1 and $N_2 = [m - 3(1 - f)]N/m$ near D2 (Fig. 4d). This equilibration process releases energy, and, to conserve the appropriate quantum numbers^{15,35,45}, they lead to the creation of neutralon excitations (quasiparticles of the neutral modes characterized by non-trivial statistics). The latter are transported upstream from the vicinity of D2 and D1 in the direction of the QPC (and the sources). Along their trajectories, they fully decay into stochastic particle–hole pairs in the adjacent charge modes (as random pulses, equally probable particles and holes)³³. The excitations in these modes near S1 and near S2 are schematically shown in Fig. 4e. Considering a fraction f of tunnelling events between the inner modes, the total charge reaching D1 is Q_{D1} (Fig. 4e and Supplementary Section IV), with average $\overline{Q_{D1}} = \frac{(1-f)Ne}{m}$. The charge fluctuations, given by the autocorrelation of Q_{D1} measured over time τ at D1, are given by $\frac{(1-f)(m-3)Ne^2}{3m^2}$. Together with the orthodox beam-partitioning contribution^{38,41} of $\frac{f(1-f)Ne^2}{m^2}$, the resulting total irreducible zero-frequency current–current autocorrelation at D1 is $\ll I_{D1}I_{D1} \gg_{\omega=0} = \frac{2(1-f)(m+3f-3)Ne^2}{3m^2\tau}$. Expressing f in terms of t , the effective

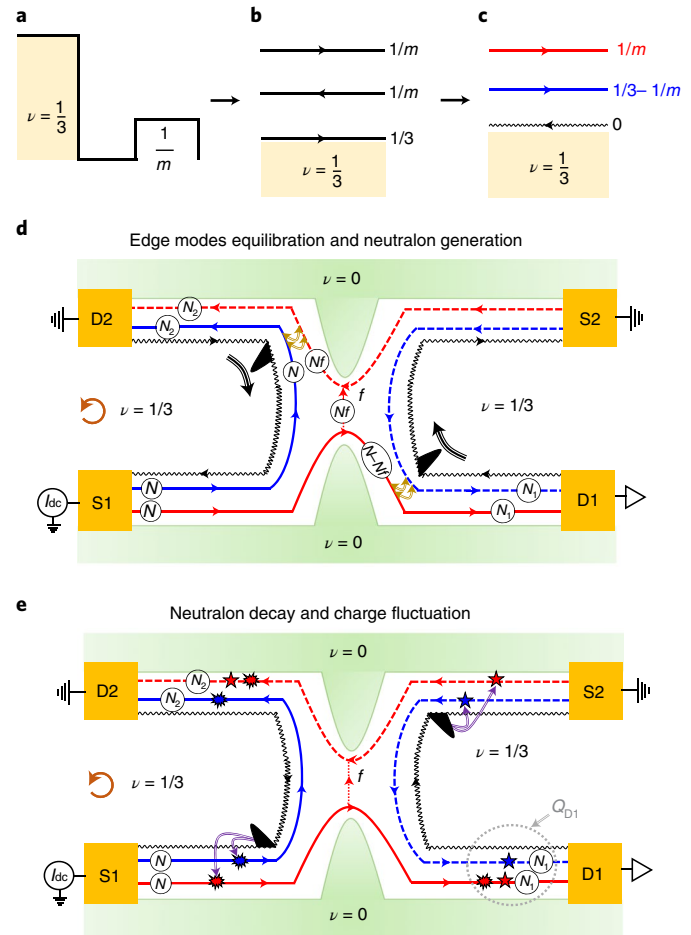


Fig. 4 | Theoretical model with the example of reconstructed $\nu = 1/3$. **a**, The electronic occupation near the edge for $\nu = 1/3$ with a $1/m$ reconstruction. **b**, The resulting bare edge modes. **c**, Renormalized edge: the outer mode remains disconnected and the two inner modes are renormalized, giving rise to a redefined DS charged mode and a counter-propagating neutral mode. The characterization of the modes, from inner to outer, is $1/3 - 1/m$ (blue) and $1/m$ (red). **d**, The QPC with bulk filling $1/3$, following $1/m$ edge reconstruction and renormalization. f is the tunnelling probability between the two $1/m$ charge modes, resulting in the charge transmitted to D1 (red). The number of charged particles (measured over a time interval τ) in the respective modes at different stages along the propagation is schematically shown in small circles. Equilibration between charge modes is shown by dark-yellowish double arrows, and the black bumps represent excitations (neutralons) in the neutral mode, which propagate upstream. **e**, Decay (shown by purple arrows) of neutralons, leading to the stochastic generation of charge (quasiparticle/quasihole) pulses near S1 (represented by ‘beetles’) and near S2 (represented by ‘stars’). All charge contributions reaching drain D1 (and the amplifier) are depicted in the big dotted circle (total charge Q_{D1}). For a quantitative analysis, see Supplementary Section IV.

Fano factor is then given by $F = \frac{\ll I_{D1}I_{D1} \gg_{\omega=0}}{2I_{\text{dc}} \times \text{ext}(1-t)} = \frac{1}{3}$. Here, the Fano factor represents the bulk filling as well as the quasiparticle charge.

The latter statement does not hold for other particle-like states, such as $\nu = 2/5$, $\nu = 3/7$, or even for particle–hole conjugated states, such as $\nu = 2/3$, $\nu = 3/5$ and $\nu = 4/7$. In Supplementary Section IV, we present a general calculation for an arbitrary filling with edge reconstruction and the ensuing renormalization leading to the emergence of neutral modes. Furthermore, we present a similar analysis for less conventional geometry with an engineered interfaced boundary. Remarkably, in all these cases, the Fano factor coincides with the bulk filling factor. We note that the Fano factor is unaffected by the partitioning of the charged quasiparticles (represented by the factor f ; Fig. 4d,e). Hence,

it retains its value for $f=0$, that is, on an intermediate conductance plateau within the QPC^{33,34}. We stress that details of the edge reconstruction are redundant as long as the filling fraction of the reconstructed side strip, $1/m$, is finite (Fig. 4). Even a minor reconstruction $1/m \ll 1$ leads to the universal result $F = \nu_e$. We note, however, that our results are compatible with the orthodox beam-partitioning mechanism for shot noise, expected in the absence of edge reconstruction (when no neutral modes emerge). We stress, though, that our analysis relies on a crucial assumption, namely, that the pulses arriving at the drain are statistically independent (cf. Supplementary Section IV). This assumption seems to work nicely in our experimental context, however unjustifiably.

At higher temperatures, the neutral excitations are known to decay²⁷, and one expects the (off-the-plateau) Fano factor to represent the quasiparticle charge^{24,27}. However, the states with a minute energy gap are fragile at higher temperatures. Moreover, the thermal Johnson–Nyquist noise contribution may dominate over the quantum contribution. Therefore, to study such exotic states, for example, $3/7$ and $5/2$, at low temperatures, a simple path for extracting this charge combines experiment and theory. We measure the noise on and off the conductance plateau, calculate the neutral mode contribution to the latter and then extract the beam-partitioning contribution to the noise off the plateau. This last contribution is a marker of the quasiparticle charge. We note, however, that $1/m$ may be exceedingly small, resulting in a blurred plateau with an elusive conclusion concerning the quasiparticle charge and the on-the-plateau noise. Further protocols and geometries are needed to determine the partitioned charge accurately.

Implications

Although this work has concentrated on quantum Hall states, its implications are much wider. For example, 2D topological insulators, with conducting edges and insulating bulk, allowing study of the topological order in the bulk (relying on bulk–edge correspondence), are not immune from the deleterious effects of spontaneous edge reconstruction. Such an unexpected effect, which depends on uncontrolled details of the tested structure, may lead to erroneous interpretation of the collected edge data. Hence, interpreting the transport along the edge requires that the edge mirrors the bulk faithfully.

Online content

Any methods, additional references, Nature Research reporting summaries, source data, extended data, supplementary information, acknowledgements, peer review information; details of author contributions and competing interests; and statements of data and code availability are available at <https://doi.org/10.1038/s41567-022-01758-x>.

References

- Laughlin, R. B. Anomalous quantum Hall effect—an incompressible quantum fluid with fractionally charged excitations. *Phys. Rev. Lett.* **50**, 1395–1398 (1983).
- Heiblum, M. Quantum shot noise in edge channels. *Phys. Status Solidi B Basic Solid State Phys.* **243**, 3604–3616 (2006).
- Ronen, Y. et al. Charge of a quasiparticle in a superconductor. *Proc. Natl Acad. Sci. USA* **113**, 1743–1748 (2016).
- Jehl, X., Sanquer, M., Calemczuk, R. & Maily, D. Detection of doubled shot noise in short normal-metal/superconductor junctions. *Nature* **405**, 50–53 (2000).
- Bastiaans, K. M. et al. Direct evidence for Cooper pairing without a spectral gap in a disordered superconductor above T_c . *Science* **374**, 608–611 (2021).
- Serlin, M. et al. Intrinsic quantized anomalous Hall effect in a moiré heterostructure. *Science* **367**, 900–903 (2019).
- Xie, Y. et al. Fractional Chern insulators in magic-angle twisted bilayer graphene. *Nature* **600**, 439–443 (2021).
- Hasan, M. Z. & Kane, C. L. Colloquium: topological insulators. *Rev. Mod. Phys.* **82**, 3045–3067 (2010).
- Prange, R. & Girvin, S. M. *The Quantum Hall Effect* (Springer, 1990).
- Sarma, S. D. & Pinczuk, A. *Perspective in Quantum Hall Effects* (Wiley, 1996).
- Halperin, B. I. & Jain, J. K. *Fractional Quantum Hall Effects: New Developments* (World Scientific, 2020).
- Halperin, B. I. Quantized Hall conductance, current-carrying edge states, and the existence of extended states in a two-dimensional disordered potential. *Phys. Rev. B* **25**, 2185–2190 (1982).
- Wen, X.-G. *Quantum Field Theory of Many-Body Systems: From the Origin of Sound to an Origin of Light and Electrons* (Oxford Univ. Press, 2004).
- Kane, C. L. & Fisher, M. P. A. in *Perspectives in Quantum Hall Effects: Novel Quantum Liquids in Low-Dimensional Semiconductor Structures* (eds Das Sarma, S. & Pinczuk, A.) Ch. 4 (Wiley, 1996).
- Wen, X. G. Gapless boundary excitations in the quantum Hall states and in the chiral spin states. *Phys. Rev. B* **43**, 11025–11036 (1991).
- Stern, A. Anyons and the quantum Hall effect—a pedagogical review. *Ann. Phys.* **323**, 204–249 (2008).
- Zheng, H. Z., Wei, H. P., Tsui, D. C. & Weimann, G. Gate-controlled transport in narrow GaAs/Al_xGa_{1-x}As heterostructures. *Phys. Rev. B* **34**, 5635–5638 (1986).
- Heiblum, M. & Feldman, D. E. Edge probes of topological order. *Int. J. Mod. Phys. A* **35**, 2030009 (2020).
- Chang, A. M. Chiral Luttinger liquids at the fractional quantum Hall edge. *Rev. Mod. Phys.* **75**, 1449–1505 (2003).
- dePicciotto, R. et al. Direct observation of a fractional charge. *Nature* **389**, 162–164 (1997).
- Saminadayar, L., Glattli, D. C., Jin, Y. & Etienne, B. Observation of the $e/3$ fractionally charged Laughlin quasiparticle. *Phys. Rev. Lett.* **79**, 2526–2529 (1997).
- Reznikov, M., de Picciotto, R., Griffiths, T. G., Heiblum, M. & Umansky, V. Observation of quasiparticles with one-fifth of an electron's charge. *Nature* **399**, 238–241 (1999).
- Dolev, M., Heiblum, M., Umansky, V., Stern, A. & Mahalu, D. Observation of a quarter of an electron charge at the $\nu=5/2$ quantum Hall state. *Nature* **452**, 829–834 (2008).
- Chung, Y. C., Heiblum, M. & Umansky, V. Scattering of bunched fractionally charged quasiparticles. *Phys. Rev. Lett.* **91**, 216804 (2003).
- Bid, A., Ofek, N., Heiblum, M., Umansky, V. & Mahalu, D. Shot noise and charge at the $2/3$ composite fractional quantum Hall state. *Phys. Rev. Lett.* **103**, 236802 (2009).
- Bhattacharyya, R., Banerjee, M., Heiblum, M., Mahalu, D. & Umansky, V. Melting of interference in the fractional quantum Hall effect: appearance of neutral modes. *Phys. Rev. Lett.* **122**, 246801 (2019).
- Bid, A. et al. Observation of neutral modes in the fractional quantum Hall regime. *Nature* **466**, 585–590 (2010).
- Inoue, H. et al. Proliferation of neutral modes in fractional quantum Hall states. *Nat. Commun.* **5**, 4067 (2014).
- Wang, J., Meir, Y. & Gefen, Y. Edge reconstruction in the $\nu=2/3$ fractional quantum Hall state. *Phys. Rev. Lett.* **111**, 246803 (2013).
- Khanna, U., Goldstein, M. & Gefen, Y. Edge reconstruction and emergent neutral modes in integer and fractional quantum Hall phases. *Low Temp. Phys.* **48**, 420–427 (2022).
- Meir, Y. Composite edge states in the $\nu=2/3$ fractional quantum Hall regime. *Phys. Rev. Lett.* **72**, 2624–2627 (1994).

32. Hu, L. & Zhu, W. Abelian origin of $\nu=2/3$ and $2+2/3$ fractional quantum Hall effect. *Phys. Rev. B* **105**, 165415 (2022).
33. Khanna, U., Goldstein, M. & Gefen, Y. Fractional edge reconstruction in integer quantum Hall phases. *Phys. Rev. B* **103**, L121302 (2021).
34. Sabo, R. et al. Edge reconstruction in fractional quantum Hall states. *Nat. Phys.* **13**, 491–496 (2017).
35. Kane, C. L., Fisher, M. P. & Polchinski, J. Randomness at the edge: theory of quantum Hall transport at filling $\nu=2/3$. *Phys. Rev. Lett.* **72**, 4129–4132 (1994).
36. Spånslätt, C., Park, J., Gefen, Y. & Mirlin, A. D. Conductance plateaus and shot noise in fractional quantum Hall point contacts. *Phys. Rev. B* **101**, 075308 (2020).
37. Lin, C. et al. Charge equilibration in integer and fractional quantum Hall edge channels in a generalized Hall-bar device. *Phys. Rev. B* **99**, 195304 (2019).
38. Martin, T. & Landauer, R. Wave-packet approach to noise in multichannel mesoscopic systems. *Phys. Rev. B* **45**, 1742–1755 (1992).
39. Buttiker, M. Scattering theory of current and intensity noise correlations in conductors and wave guides. *Phys. Rev. B* **46**, 12485–12507 (1992).
40. Feldman, D. E. & Heiblum, M. Why a noninteracting model works for shot noise in fractional charge experiments. *Phys. Rev. B* **95**, 115308 (2017).
41. Dolev, M. et al. Dependence of the tunneling quasiparticle charge determined via shot noise measurements on the tunneling barrier and energetics. *Phys. Rev. B* **81**, 161303 (2010).
42. Comforti, E., Chung, Y. C., Heiblum, M., Umansky, V. & Mahalu, D. Bunching of fractionally charged quasiparticles tunnelling through high-potential barriers. *Nature* **416**, 515–518 (2002).
43. Chamon, C. & Wen, X. G. Sharp and smooth boundaries of quantum Hall liquids. *Phys. Rev. B* **49**, 8227–8241 (1994).
44. Khanna, U., Murthy, G., Rao, S. & Gefen, Y. Spin mode switching at the edge of a quantum Hall system. *Phys. Rev. Lett.* **119**, 186804 (2017).
45. Park, J., Rosenow, B. & Gefen, Y. Symmetry-related transport on a fractional quantum Hall edge. *Phys. Rev. Res.* **3**, 023083 (2021).

Publisher's note Springer Nature remains neutral with regard to jurisdictional claims in published maps and institutional affiliations.

Springer Nature or its licensor holds exclusive rights to this article under a publishing agreement with the author(s) or other rightsholder(s); author self-archiving of the accepted manuscript version of this article is solely governed by the terms of such publishing agreement and applicable law.

© The Author(s), under exclusive licence to Springer Nature Limited 2022

Data availability

Data related to this paper are available from the corresponding author upon reasonable request. Source data are provided with this paper.

Acknowledgements

We acknowledge discussions with I. Gornyi. In particular, we are indebted to A. Mirlin for pointing out the difficulty with our assumption of independent pulses arriving at the drain. We acknowledge the continuous support of the Sub-Micron Center staff. M.H. acknowledges support from the European Research Council under the European Community's Seventh Framework Programme (FP7/2007–2013)/ERC under grant agreement no. 713351, partial support of the Minerva Foundation with funding from the Federal German Ministry for Education and Research (grant no. 713534). M.G. was supported by the Israel Science Foundation and the Directorate for Defense Research and Development grant no. 3427/21 and by the US–Israel Binational Science Foundation (grants nos. 2016224 and 2020072). Y.G. was supported by CRC 183 (project C01), the Minerva Foundation, DFG grant no. RO 2247/11-1, MI 658/10-2, the German–Israeli Foundation (grant no. I-118-303.1-2018), the National Science Foundation (award DMR- 2037654) and the US–Israel Binational Science Foundation, and the Helmholtz International Fellow Award. A.D. was supported by the German–Israeli Foundation (grant no. I-1505-303.10/2019). A.D. also thanks the Koshland Foundation for a Koshland Fellowship, the Israel Planning and Budgeting Committee and Weizmann Institute of Science, Israel Dean of Faculty fellowship for financial support.

Author contributions

S.B. and R.B. fabricated the devices, performed the measurements and analysed the data with H.K.K. M.H. supervised the experiment and the analysis. Y.G. contributed to conceiving the theoretical model. A.D., M.G. and Y.G. developed the theoretical model. V.U. grew the GaAs heterostructures. All authors contributed to the writing of the manuscript.

Competing interests

The authors declare no competing interests.

Additional information

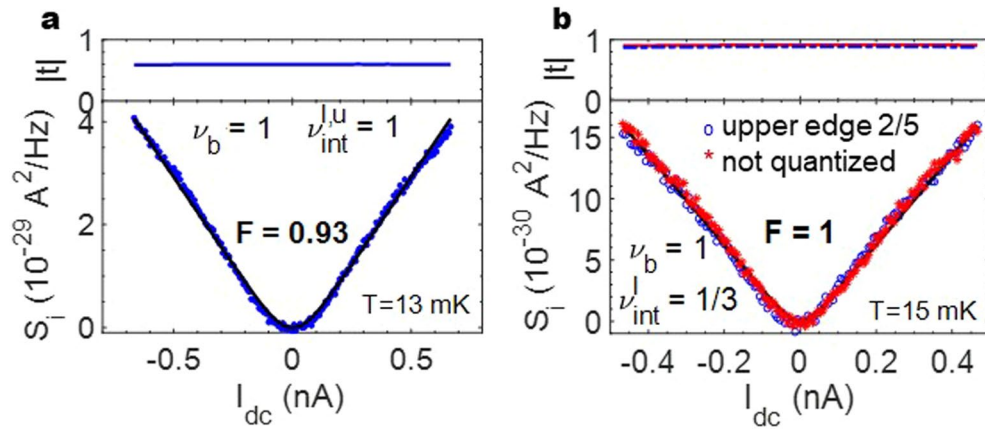
Extended data is available for this paper at <https://doi.org/10.1038/s41567-022-01758-x>.

Supplementary information The online version contains supplementary material available at <https://doi.org/10.1038/s41567-022-01758-x>.

Correspondence and requests for materials should be addressed to Moty Heiblum.

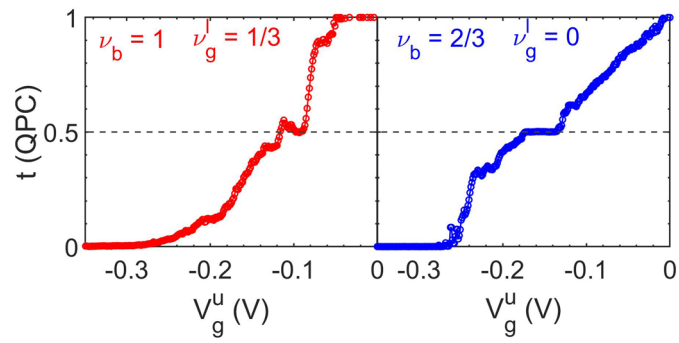
Peer review information *Nature Physics* thanks the anonymous reviewers for their contribution to the peer review of this work

Reprints and permissions information is available at www.nature.com/reprints.



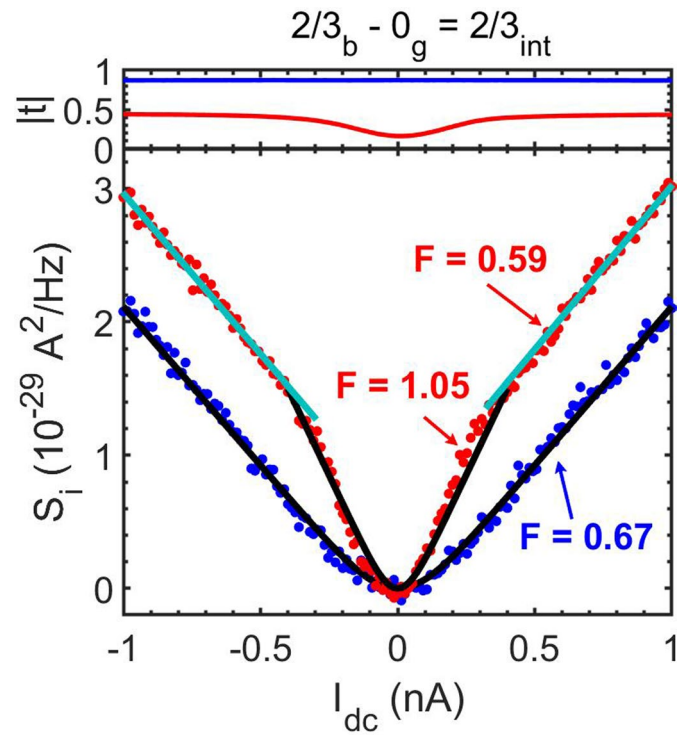
Extended Data Fig. 1 | Shot noise at integer bulk $\nu_b = 1$ with symmetric and asymmetric QPC. a, Downstream current noise (S_i) at bulk filling factor $\nu_b = 1$ for the regular case, that is, when both the upper and lower modes are $\nu_{\text{int}}^{l,u} = 1$. Fano factor is $F = 0.93$. **b**, S_i when the partitioned edge is $1_b - 2/3_g = 1/3_{\text{int}}$, and the QPC

is asymmetric with $\nu_g^l \neq \nu_g^u$ and ν_g^u not quantized. Obtained $F = 1$, with an accuracy of ± 0.05 . The electron temperature is slightly higher (about 3–4 mK) than the fridges' base temperature.



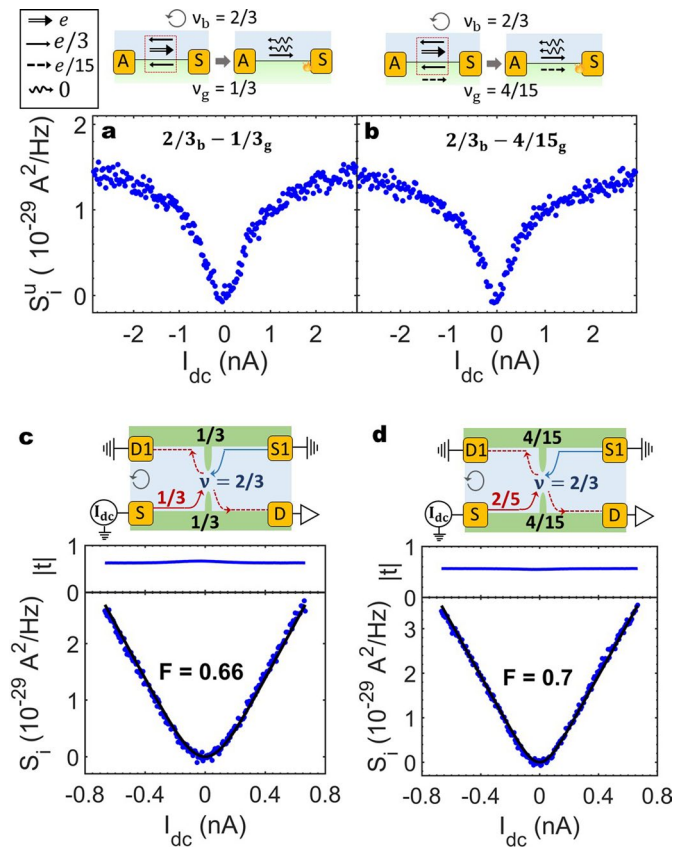
Extended Data Fig. 2 | QPC transmission for two types of interface $2/3$ modes: $1 - 1/3$ and $2/3 - 0$. QPC transmission as a function of upper-gate voltage V_g^u when the incoming mode at the lower bulk-gate interface is $1_b - 1/3_g = 2/3_{\text{int}}$ (left)

and $2/3_b - 0_g = 2/3_{\text{int}}$ (right). The transmission shows a plateau at $t = 1/2$ for both cases, indicating edge reconstruction.



Extended Data Fig. 3 | Quasiparticle bunching at strong backscattering of $2/3 - 0$ edge mode. Quasiparticle bunching leads to electron tunneling with $F \cong 1$ at low QPC transmission and small impinging bias current (red plots). At a higher bias current, the transmission increases and the Fano factor becomes

close to $2/3$. This is consistent with the result of $2/3$ edge in a regular QPC (Ref. 25). For the comparison, shot noise with $F \cong 2/3$ at a higher transmission over the full bias current range is also shown (blue plots).



Extended Data Fig. 4 | Upstream noise and Fano factor for newly engineered fractional states $2/3 - 1/3 = 1/3$ and $2/3 - 4/15 = 2/5$. **a,b**, Spectral density of upstream current noise, measured at an upstream amplifier $70 \mu\text{m}$ distant from the source hot-spot. Unlike ubiquitous $1/3$ and $2/5$ modes, the interface $2/3_b - 1/3_g = 1/3_{\text{int}}$ and $2/3_b - 4/15_g = 2/5_{\text{int}}$ modes are expected to have negative or zero thermal conductance (K_{xy}); hence, they carry topological neutral modes. Note that $4/15$ is a new quantum Hall state, which we could stabilize only by

gating in a few bulk-gate devices. **c,d**, Spectral density of downstream current noise for $1/3_{\text{int}}$ at $t \approx 0.63$ and for $2/5_{\text{int}}$ at $t \approx 0.56$ when the QPC is set at symmetric configuration. Blue dots are the measured data and black solid lines are the fit. Estimated Fano factors are close to $2/3$, the bulk filling factor. Schematics in the respective inset describe the interface mode incident on the QPC and the corresponding bulks.